Slightly Tapered Optical Fiber with Inner Air-cavity for Simultaneous Refractive Index and Temperature Sensing

D.N.Wang[1], Lei Zhang[2], Jibing Liu[3] and H. F. Chen[1]
[1]*College of Optical and Electronic Technology, China Jiliang University, Hangzhou, China*
[2]*Department of Electrical Engineering, Hubei Polytechnic University, Huangshi, China*
[3]*College of Physics and Electronic Science, Hubei Normal University, Huangshi, China*

Keywords: Optical Fiber Sensors, Interferometry, Microstructure Fabrication.

Abstract: A fiber in-line Mach-Zehnder interferometer based on inner air-cavities for simultaneous refractive index and temperature sensing is presented. The inner air-cavities are fabricated by use of femtosecond laser micromachining, fusion splicing and slightly tapering techniques. The transmission spectrum of the interferometer exhibits a number of resonance wavelength dips corresponding to different orders of cladding modes. By tracking the shift of two dip wavelengths, the changes of refractive index and temperature can be obtained by use of a matrix method. The refractive index and temperature sensitivity achieved are 103.00 nm/RIU (refractive index unit) and 73.07 pm/℃, respectively.

1 INTRODUCTION

A simultaneous refractive index (RI) and temperature sensing is of great importance for many applications in chemical industry, environmental monitoring and biological sensing. One of the techniques is to use optical fiber sensors because of their convenient operation and many advantages provided by optical fibers. A wide range of optical fiber sensor configurations have been proposed, such as the use of slanted multimode fiber Bragg grating (FBG) (Zhao et al.), sampled FBG (Shu et al.), birefringent FBG (Frazão et al.) cascaded long period gratings (Zhang et al.), hybrid gratings (Chen et al.), and different types of optical fiber interferometers with hybrid structures (Kim et al.; Lu et al.; Choi et al.; Li et al.; X. Chen et al.; Liao et al.; Xiong et al.; Yao et al.; Meng et al.). The above mentioned systems commonly are complex in design, difficult in fabrication and of high cost. Moreover, the sensor heads are large in size, which makes it difficult to precisely determine the sensing location.

Here we demonstrate a fiber in-line MZI based on inner air-cavities for simultaneous RI and temperature measurement. The proposed sensor is formed by creating an inner air-cavity by use of femtosecond (fs) laser micromachining together with fusion splicing technique and followed by a slightly tapering process (F. Chen et al.) The RI and temperature can be simultaneously determined by use of standard matrix inversion method. The sensitivities achieved are 103.00 nm/RIU (refractive index unit) and 73.07 pm/°C, respectively. The device is robust, easy in operation and has high sensitivity.

2 DEVICE FABRICATION AND OPERATION PRINCIPLE

2.1 Device Fabrication

Fig. 1 shows the microscope image of the device sensor head, fabricated by creating an inner-cavity by fs laser micromachining together with fusion splicing technique and then followed by a slightly tapering process. The length and width of the air-cavity inside the single mode fiber (SMF) are ~62 and ~80 μm, respectively. During the device fabrication process, firstly, the fs laser pulses (800 nm) with pulse width of ~120 fs and energy of ~3 μJ at the repetition rate of 1 kHz were focused onto a cleaved single mode fiber (SMF) by a 20× objective lens with a numerical aperture (NA) value of 0.50. The SMF was mounted on a computer controlled X-

Wang, D., Zhang, L., Liu, J. and Chen, H.
Slightly Tapered Optical Fiber with Inner Air-cavity for Simultaneous Refractive Index and Temperature Sensing.
DOI: 10.5220/0005964900480052
In *Proceedings of the 13th International Joint Conference on e-Business and Telecommunications (ICETE 2016) - Volume 3: OPTICS*, pages 48-52
ISBN: 978-989-758-196-0

Y-Z translation stage with a 40 nm resolution. A micro-hole with a diameter of ~12 μm and depth of ~25 μm was created at the center of the cleaved fiber end facet. Secondly, a cleaved SMF without a micro-hole was used to fusion splice the fiber tip with a micro-hole. An inner air-cavity was created due to the extremely high heating temperature. The fusion splicer used was ERICSSON FSU975, and the fusing current and fusing duration employed were 16.2 mA and 2.0 s, respectively. Lastly, the SMF with an inner air-cavity was slightly tapered by using flame brushing technique to effectively excite cladding mode in the optical fiber.

2.2 Principle of Operation

The schematic diagram of the sensor head is illustrated in Fig. 2. The light launched into the inner air-cavity is split into two parts: one passes through the air-cavity and the other travels along the fiber cladding. Finally, the interference is formed since both of the two beams are recombined at the end of air-cavity. The output of the MZI is given by

$$I = I_a + I_c + 2\sqrt{I_a I_c}\cos(\frac{2\pi L\Delta n}{\lambda}) \quad (1)$$

where I_a and I_c represent the intensity of the light passing through the air-cavity and traveling along the fiber cladding, respectively, λ is the wavelength, L is the cavity length, and $\Delta n = n_c - n_a$ is the effective RI difference between the air-cavity mode and the cladding mode. When the phase term satisfies the condition: $2\pi L\Delta n/\lambda = (2m+1)\pi$, where m is an integer, the intensity dip appears at the wavelength

$$\lambda_{dip} = \frac{2L\Delta n}{2m+1} \quad (2)$$

The temperature sensitivity at λ_{dip} can be written as

$$\frac{\partial\lambda_{dip}}{\partial T} = \frac{2}{2m+1}[\Delta n\frac{\partial L}{\partial T} + L(\frac{\partial n_c}{\partial T} - \frac{\partial n_a}{\partial T})] \quad (3)$$

where T is the temperature. Assuming the thermo-expansion coefficient is α and thermo-optical coefficient is ξ , where $\partial L/\partial T = \alpha L$ and $\partial n_c/\partial T = n_c\xi$. Since the effective RI of air-cavity is nearly a constant, $\partial n_a/\partial T = 0$. Eq. (2) can be simplified as

$$\frac{\partial\lambda_{dip}}{\partial T} = \frac{2L}{2m+1}[\Delta n\alpha + n_c\xi] \quad (4)$$

The temperature sensitivity is mainly dependent on the second term in Eq. (4) as the thermal-optical coefficient ξ is much larger than the thermo-expansion coefficient α in silica. For different transmission modes in cladding, since the effective RI and effective thermo-optical coefficient vary with the mode order, the temperature sensitivities of different mode orders are different.

Similarly, we can derive the dip wave shift due to the change of RI of environment as

$$\frac{\partial\lambda_{dip}}{\partial\psi} = \frac{2L}{2m+1}[\frac{\partial n_c}{\partial\psi} - \frac{\partial n_a}{\partial\psi}] \quad (5)$$

where ψ is the applied RI at the sensor device.

The transmission spectra of the device in air and water respectively, are shown in Fig. 3, where four dips appear. The two dips located at 1481.23 nm and 1580.63 nm in the water are selected for simultaneously RI and temperature sensing. We employ a matrix to present the dip wavelength shift corresponding to the variation of RI of environment and of temperature,

$$\begin{bmatrix}\Delta\lambda_1\\ \Delta\lambda_2\end{bmatrix} = \begin{bmatrix}j_1 & k_1\\ j_2 & k_2\end{bmatrix}\begin{bmatrix}\Delta T\\ \Delta\psi\end{bmatrix} \quad (6)$$

where $\Delta\lambda_1$ and $\Delta\lambda_2$ are the wavelength shifts, j_1 and j_2 represent the temperature sensitivities, and k_1 and k_2 are the RI sensitivities of dip 1 and dip 2, respectively. ΔT and $\Delta\psi$ denote the variation of temperature and RI applied onto the sensor, respectively.

3 EXPERIMENTAL RESULTS AND DISCUSSIONS

To test the proposed device, the experimental set-up as shown in Fig. 4 was used. The sensor head was mounted between two fixed stages. The temperature was controlled by a column oven with an accuracy of ±0.1□. To test the system response to the RI change, the sensor head was immersed into a series of RI liquids (from Cargille Laboratories), and after each measurement, the fiber sensor head was rinsed with methanol carefully until no residue liquid was left on the sensor head surface and the original spectrum could be restored. The fiber device was

connected to a broadband source (BBS) and an optical spectrum analyzer (OSA: YOKOGAWA 6390) with 0.01 nm resolution. When the RI and temperature were changed, the wavelength shifts of dip 1 and dip 2 were recorded by the OSA.

To test the thermal response of the two dips, the device was heated from 25 to 65°C with a step of 5°C in the air. As shown in Fig. 5, both the dip wavelengths increase with the elevated temperature. After employing linear fit to the experimental data, the temperature responses of the two dips were depicted in the Fig. 6. The sensitivities obtained are 73.07 pm/°C and 67.07 pm/°C, respectively.

The RI sensitivities were calibrated at the room temperature of ~23°C, and tested within the range between 1.33 and 1.38. As shown in Fig. 7, both the dip wavelengths decrease with the increase of RI. After employing linear fit to the experimental data, the RI responses of the two dips were depicted in Fig. 8. The RI sensitivities k_1 and k_2 obtained are -103.00 and -78.94 nm/RIU, respectively.

According to the separate temperature and RI measurements, the matrix in Eq. (6) can be written as

$$\begin{bmatrix} \Delta\lambda_1 \\ \Delta\lambda_2 \end{bmatrix} = \begin{bmatrix} 0.07307 & -103.00 \\ 0.06707 & -78.94 \end{bmatrix} \begin{bmatrix} \Delta T \\ \Delta\psi \end{bmatrix} \quad (7)$$

By employing the matrix inversion method, we can derive the change of temperature and RI on the fiber device as

$$\begin{bmatrix} \Delta T \\ \Delta\psi \end{bmatrix} = \begin{bmatrix} -69.2417 & 90.3458 \\ -0.0588 & 0.0641 \end{bmatrix} \begin{bmatrix} \Delta\lambda_1 \\ \Delta\lambda_2 \end{bmatrix} \quad (8)$$

where the units of ΔT and $\Delta\psi$ are in °C and RIU, respectively, and that of $\Delta\lambda_1$ and $\Delta\lambda_2$ are in nm. Then, we can obtain the temperature and RI information simultaneously as $T_r + \Delta T$ and $\psi_r + \Delta\psi$, where T_r and ψ_r are reference parameters, such as the parameters of room temperature and the RI of water.

In the experiments, since the temperature was controlled by a column oven, the fluctuation is around ±0.1°C. Due to the 0.01 nm resolution of the OSA, the RI and temperature resolutions can be estimated to be ~9.7×10^{-5}RIU and ~0.14°C, respectively. Our proposed sensor head demonstrates high sensitivity in RI (-103.00 nm/RIU) and temperature (73.07 pm/°C). Moreover, since the size of MZI cavity is 62 μm, the sensing location can be precisely determined.

The inner air-cavity itself also forms a Fabry-Perot (FP) cavity, the corresponding free spectral range (FSR) should be ~19.4 nm, however, according to Fig. 3, the FSR of the fringe pattern obtained is ~64.4 nm. Obviously, the FP effect can be ignored.

4 CONCLUSIONS

In conclusion, we have proposed and demonstrated a fiber in-line MZI based on inner air-cavities for simultaneous RI and temperature sensing. The proposed optical fiber sensor is ultra compact in size, simple in structure and precise in sensing location. The achieved refractive index and temperature sensitivities are -103.00 nm/RIU and 73.07 pm/°C, respectively. Such a sensing device has high potential in chemical, environmental and biological sensing applications.

ACKNOWLEDGEMENTS

This work was supported in part by National Natural Science Foundation of China (61377094 and 61290313).

REFERENCES

C. L. Zhao, X. F. Yang, M. S. Demokan, and W. Jin, "Simultaneous temperature and refractive index measurements using a 3o slanted multimode fiber Bragg grating, " *J. Lightw. Technol.*, 24, 879-883.

Shu, B. A. L. Gwandu, Y. Liu, L. Zhang, and I. Bennion, "Sampled fiber Bragg grating for simultaneous refractive-index and temperature measurement," *Opt. Lett.*, 26, 774–776.

O. Frazão, B. V. Marques, P. Jorge, J. M. Baptista, and J. L. Santos, "Higher birefringence D-type fiber loop mirror used as refractometer, " *Sens. Actuators B, Chem.*, 135, 108-111.

A. P. Zhang, L. Y. Shao, J. F. Ding, and S. L. He, "Sandwiched long-period gratings for simultaneous measurement for refractive index and temperature, " *IEEE Photon. Technol. Lett.*, 17, 2397-2399.

X. Chen, K. Zhou, L. Zhang, and I. Bennion, "Simultaneous measurement of temperature and external refractive index by use of a hybrid grating in D fiber with enhanced sensitivity by HF etching," *Appl. Opt.*, 44, 178–182.

D. W. Kim, F. Shen, X. Chen, and A. Wang, "Simultaneous measurement of refractive index and temperature based on a reflectionmode long-period grating and an intrinsic Fabry-Perot interferometer sensor," *Opt. Lett.*, 30, 3000–3002.

P. Lu, L. Men, K. Sooley, and Q. Chen, "Tapered fiber Mach-Zehnder interferometer for simultaneous measurement of refractive index and temperature," *Appl. Phys. Lett.*, 94, 131110-1–131110-3.

Hae Young Choi, Gopinath Mudhana, Kwan Seob Park, Un-Chul Paek, and Byeong Ha Lee, "Cross-talk free and ultra-compact fiber optic sensor for simultaneous measurement of temperature and refractive index, " *Opt. Exp.*, 18, 141-149.

L.C. Li, X. Li, Z.H. Xie, Z.L. Liao, F. Tu, D. M. Liu, "Simultaneous measurement of refractive index and temperature using thinned fiber based Mach-Zehnder interferometer, " *Opt. Comm.*, 285, 3945-3949.

L. X. Chen, X. G. Huang, J. Y. Li, and Z. B. Zhong, "Simultaneous measurement of refractive index and temperature by integrating an external Fabry-Perot cavity with fiber Bragg grating," *Rev. Sci. Instrum.*, 83, 053113.

C. R. Liao, Ying Wang, D. N. Wang and M. W. Yang, "Fiber In-line Mach-Zehnder interferometer embedded in FBG for simultaneous refractive index and temperature measurement," *IEEE Photon. Technol. Lett.*, 22, 1686-1688.

R. Xiong, H.Y. Meng, Q. Q. Yao, B. Huang, Y.M. Liu, H.C. Xue, C.H. Tan, and X.G. Huang, "Simultaneous measurement of refractive index and temperature based on modal interference", *IEEE Sens. J.*, 14, 2524-2528.

Q. Q. Yao, H.Y. Meng, W. Wang, H.C. Xue, R. Xiong, B. Huang, C.H. Tan, X. G. Huang, "Simultaneous measurement of refractive index and temperature based on a core-offset Mach-Zehnder interferometer combined with a fiber Bragg grating", *Sens. Actuators A, Phy.*, 209, 73-77.

H.Y. Meng, W. Shen, G. B. Zhang, C. H. Tang and X. G. Huang, "Fiber Bragg grating-based fiber sensor for simultaneous measurement of refractive index and temperature", *Sens. Actuators B, Chem.*, 150, 226-229.

H. F. Chen, D. N. Wang and W. Hong, "Slightly tapered optical fiber with inner air-cavity as a miniature and versatile sensing device", *IEEE J. Lightwave Technol.*, 33, 62-68.

APPENDIX

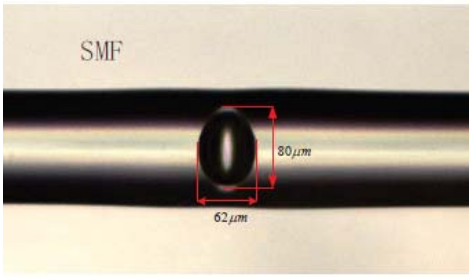

Figure 1: Microscope image of the optical fiber sensor head.

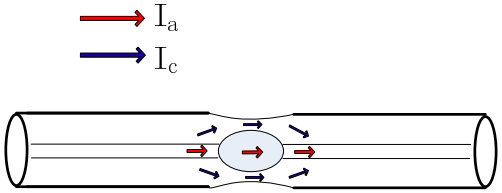

Figure 2: Schematic diagram of the sensor head.

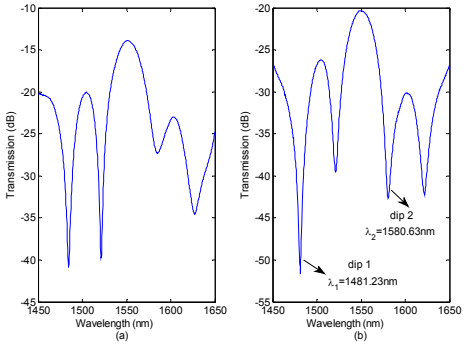

Figure 3 (a): Transmission spectrum of the sensor in air. (b) Transmission spectrum of the sensor in water.

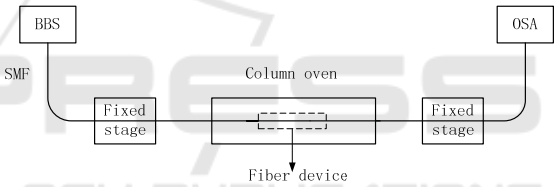

Figure 4: Experimental set-up.

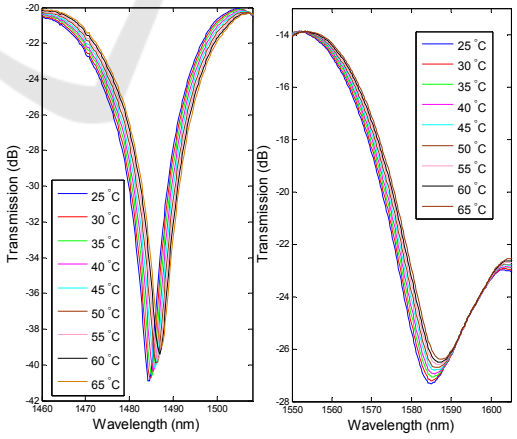

Figure 5: Dip wavelength shift with temperature.

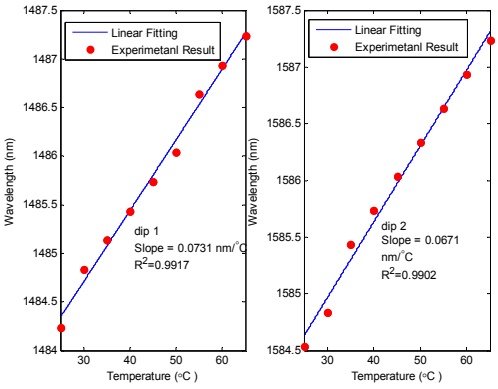

Figure 6: Dip wavelength shift with temperature by linear fitting.

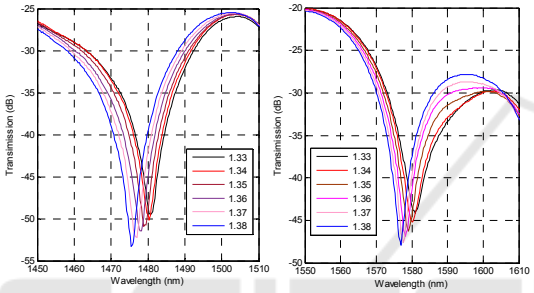

Figure 7: Dip wavelength shift with RI.

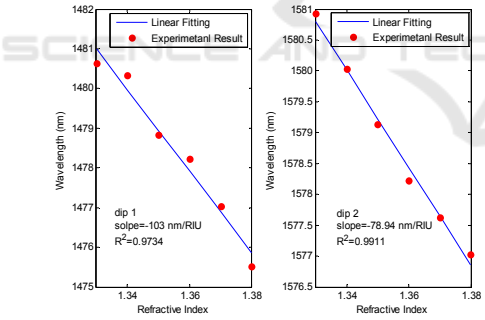

Figure 8: Dip wavelength shift with RI by linear fitting.